By Design: A Macrocyclic 3d−4f Single-Molecule Magnet with Quantifiable Zero-Field Slow Relaxation of Magnetization

Humphrey L. C. Feltham,[†] Rodolphe Clérac,[‡,§] Liviu Ungur,[⊥] Liviu F. Chibotaru,[‖] Annie K. Powell,[#,∇] and Sally Brooker*,[†]

[†]Department of Chemistry and the MacDiarmid Institute, University of Otago, P.O. Box 56, Dunedin 9054, New Zealand

[‡]CNRS, CRPP, UPR 8641, F-33600 Pessac, France

[§]Univ. Bordeaux, CRPP, UPR 8641, F-33600 Pessac, France

[‖]Division of Quantum and Physical Chemistry, Katholieke Universiteit Leuven, Celestijenlaan 200F, 3001, Leuven, Belgium
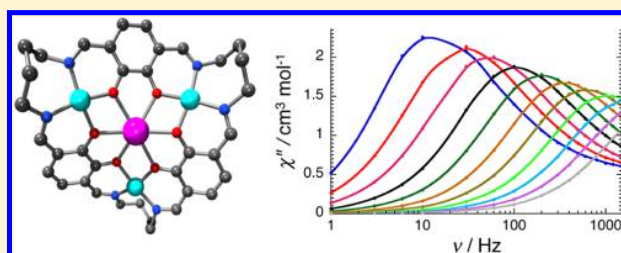
[⊥]INPAC-Institute of Nanoscale Physics and Chemistry Katholieke Universiteit Leuven, Celestijenlaan 200F, 3001, Leuven, Belgium

[#]Institut für Anorganische Chemie, Karlsruhe Institute of Technology, Engesserstrasse 15 Geb. 30.45, D76131 Karlsruhe, Germany

[∇]Institute of Nanotechnology, Karlsruhe Institute of Technology, Hermann-von-Helmholtzplatz 1, D76344 Eggenstein-Leopoldshafen, Germany

S *Supporting Information*

ABSTRACT: Rational modification of the equatorially bound tetranucleating macrocycle in the previously reported SMM complex of the propylene linked macrocycle $[Cu^{II}_3Tb^{III}(L^{Pr})](NO_3)_2$, to a new butylene linked analogue, is shown to tune the ligand field imposed on the encapsulated $Cu^{II}_3Tb^{III}$ cluster. This results in apical binding of two, rather than one, nitrate ions to the oblate Tb^{III} ion, giving enhanced uniaxial anisotropy and SMM properties despite the low symmetry of the Tb(III) site. The resulting complex, $[Cu^{II}_3Tb^{III}(L^{Bu})(NO_3)_2(MeOH)(H_2O)](NO_3 \cdot 3H_2O)$, is the first example of a macrocyclic 3d−4f single-molecule magnet that exhibits quantifiable relaxation of magnetization in zero dc field ($\Delta_{eff}/k_B = 19.5(5)$ K; $\tau_0 = 3.4 \times 10^{-7}$ s). This SMM complex of this new, larger, tetranucleating macrocycle was prepared by the template method from the 3:3:3:1 reaction of 1,4-diformyl-2,3-dihydroxybenzene/diaminobutane/copper(II) acetate/terbium(III) nitrate. Similarly, the analogues, $Zn_3Tb(L^{Bu})(NO_3)_3 \cdot MeOH \cdot H_2O \cdot DMF$ and $[Cu_3La(L^{Bu})(NO_3)_2(MeOH)(H_2O)_2](NO_3 \cdot H_2O \cdot DMF$, were prepared in order to facilitate the detailed magnetic analysis. Both copper(II) complexes were also structurally characterized, confirming the expected binding mode: lanthanide(III) ion in the central O_6 pocket, and the three copper(II) ions in the outer N_2O_2 pockets.

■ INTRODUCTION

Single-molecule magnets (SMMs) are compounds in which the individual molecules act as superparamagnetic entities.[1] As such, they exhibit magnetic properties analogous to traditional bulk magnets, but on a molecular scale, so they have attracted interest as potential components for ultradense data storage and quantum computing.[1b] At low temperatures, the magnetization of an SMM can be retained because of an energy barrier (Δ) between the all "up" and all "down" spin alignment, which, in the absence of quantum tunneling, makes moving between these two states sluggish as it requires populating high-energy intermediate states.

Hundreds of SMMs are now known.[2] A common, and successful, method of preparation is serendipitous self-assembly,[3] where various acyclic ligands and metal ions are mixed in varying ratios and left to self-assemble and crystallize out as a coordination cluster.[2a] An alternative approach is to employ macrocyclic ligands with designed binding pockets in order to gain predictability and control over the nuclearity and structure of the resulting complex, and to facilitate subsequent fine-tuning of the magnetic properties. A leading example of this approach is the use of phthalocyanine macrocycles to "sandwich" a lanthanide ion, generating families of SMMs, developed by Ishikawa et al.[2f]

We expanded on this approach by designing macrocycles large enough to provide binding pockets to accommodate 3d *and* 4f ions (Figure 1),[4] and thereby accessed the first macrocyclic 3d−4f SMM, $[Zn_3Dy(L^{Pr})]$.[4a] Nabeshima and Kajiwara reported the second such SMM, $[Zn_3Er(L^{Ph})]$.[5] More recently, we reported families of 13 $[Zn_3Ln(L^{Pr})]$[4b] and 13 $[Cu_3Ln(L^{Pr})]$[4d] complexes, as well as the first example of such a complex to show SMM behavior without application of a dc
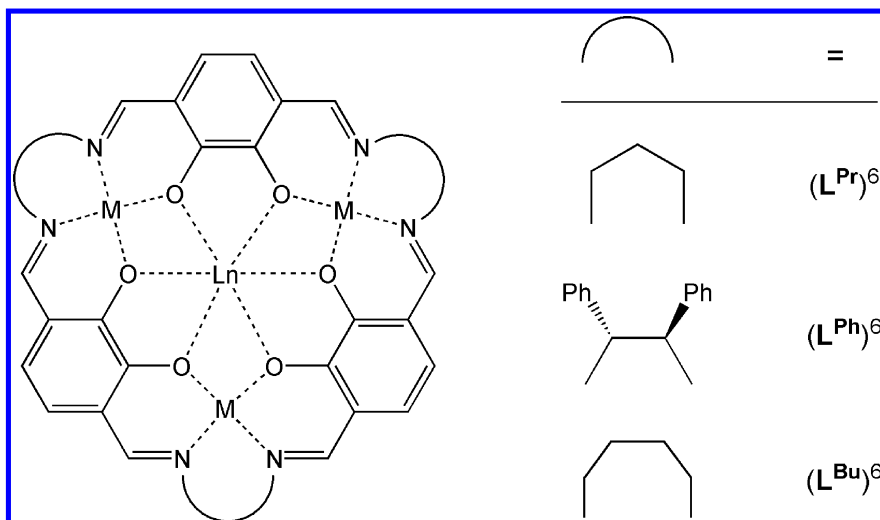
Figure 1. Schematic of the [M₃Ln] complexes with the hexaimine macrocycle (**L^{Bu}**)$^{6-}$ used in this work and of the analogues (**L^{Pr}**)$^{6-}$ and (**L^{Ph}**)$^{6-}$.

field, [Cu₃Tb(**L^{Pr}**)], albeit still without maxima in the χ'' versus ν plots.[4c]

Here, we report that improved SMM behavior can be obtained by rationally modifying the [3 + 3] Schiff base macrocycle used in [Cu₃Tb(**L^{Pr}**)].[4c] Modifying the equatorial field imposed, by increasing the ring size from 33 atoms in (**L^{Pr}**)$^{6-}$ to 36 in (**L^{Bu}**)$^{6-}$ (Figure 1), results in the first macrocyclic 3d–4f SMM to display quantifiable slow relaxation of magnetization in zero dc field, [Cu₃Tb(**L^{Bu}**)].

■ RESULTS AND DISCUSSION

Pure [Cu^{II}₃Tb^{III}(**L^{Bu}**)(NO₃)₂(MeOH)(H₂O)](NO₃)·3H₂O (referred to from here on as [Cu₃Tb(**L^{Bu}**)]) is obtained as a green solid; the analogues, Zn₃Tb(**L^{Bu}**)-(NO₃)₃·MeOH·H₂O·DMF ([Zn₃Tb(**L^{Bu}**)]) and [Cu₃La(**L^{Bu}**)-(NO₃)₂(MeOH)(H₂O)₂](NO₃)·H₂O·DMF ([Cu₃La(**L^{Bu}**)]), were also prepared to facilitate detailed magnetic analysis. Single crystals of [Cu₃Tb(**L^{Bu}**)] and [Cu₃La(**L^{Bu}**)] were obtained as [Cu₃Tb(**L^{Bu}**)(NO₃)₂(DMF)(H₂O)](NO₃)·DMF (Figure 2) and [Cu₃La(**L^{Bu}**)(NO₃)₂(MeOH)₃](NO₃) (Figure S1, Supporting Information), respectively. As expected,[4] in both cases, the large and harder lanthanide(III) ion is coordinated in the central O₆ cavity while the smaller softer copper(II) ions are bound in the outer N₂O₂ pockets. In [Cu₃Tb(**L^{Bu}**)(NO₃)₂(DMF)(H₂O)](NO₃)·DMF, the terbium-(III) ion is 10-coordinate, with distorted decahexahedral geometry, while two of the copper(II) ions are fairly regular[6] square pyramids (τ/apical molecule: Cu(2) = 0.15/H₂O; Cu(3) = 0.14/DMF) and the third is square-planar. *Two* nitrate anions are η^2-bound to the terbium(III) ion, while the third nitrate anion is not coordinated. The macrocycle is quite curved: the angles made by the plane of an arbitrarily chosen catecholate ring with the planes of the other two rings are 36.2° and 33.0°.

The magnetic properties of the complexes were investigated. For [Cu₃Tb(**L^{Bu}**)], the χT product at room temperature (RT) is 13.9 cm³ K mol⁻¹, in reasonable agreement with the expected value (12.94 cm³ K mol⁻¹) for three uncorrelated Cu^{II} ($S = {}^1\!/_2$; $g = 2.0$; $C = 0.375$ cm³ K/mol) ions and one Tb^{III} ion ($S = 3$, $L = 3$, $^7F_6$, $g = {}^3\!/_2$, $C = 11.815$ cm³ K/mol). At RT, [Zn₃Tb(**L^{Bu}**)] and [Cu₃La(**L^{Bu}**)] have χT values of 12.6 and 1.4 cm³ K mol⁻¹, respectively, in good agreement with the expected values of the
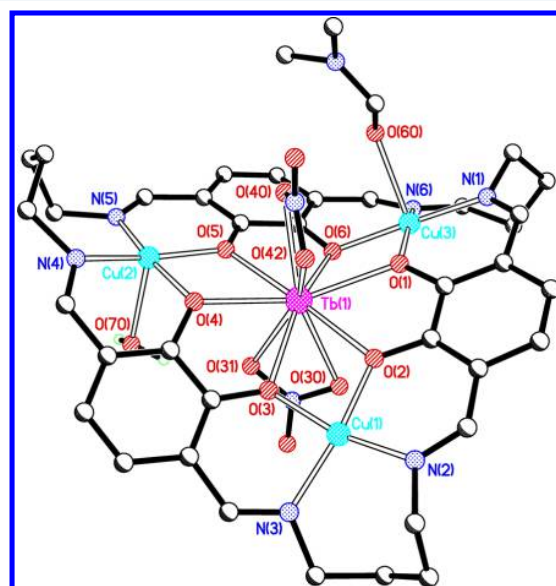

Figure 2. Crystal structure of [Cu₃Tb(**L^{Bu}**)(NO₃)₂(DMF)(H₂O)]-(NO₃)·DMF. For clarity, hydrogen atoms other than those on the water molecule and the noncoordinated nitrate anion have been omitted.

individual ion contributions (11.81 and 1.13 cm³ K mol⁻¹). For [Cu₃La(**L^{Bu}**)], the temperature dependence of χT was modeled using a simple symmetrical triangle model as a first approximation (Figure S2, Supporting Information). In keeping with the structural motif, the Heisenberg spin Hamiltonian can be written as $H = -2J(S_1 \cdot S_2 + S_1 \cdot S_3 + S_2 \cdot S_3)$. Application of the van Vleck equation[7] allows a determination of the low-field ($\mu_B H/k_B T \ll 1$) analytical expression of the magnetic susceptibility. An excellent fit of the experimental data is obtained with this theoretical susceptibility, with $J/k_B = +0.35(1)$ K and $g = 2.25(5)$, down to 1.8 K (Figure S3, Supporting Information). This result indicates weak ferromagnetic coupling between the Cu^{II} ions within [Cu₃La(**L^{Bu}**)] and hence an $S = {}^3\!/_2$ spin ground state as already observed in the analogous [Cu₃La(**L^{Pr}**)] complex.[4c]

The temperature dependence of χT for $[Cu_3Tb(L^{Bu})]$ is governed by the thermal depopulation of excited sublevels of the Tb^{III} ion and the 3d−4f and 3d−3d exchange interactions. It is usually not trivial to determine the relative contributions of each, but in our case, the fact that the analogues $[Zn_3Tb(L^{Bu})]$ and $[Cu_3La(L^{Bu})]$ can be prepared permits a qualitative investigation of these effects. Subtracting the χT versus T data for $[Zn_3Tb(L^{Bu})]$ and $[Cu_3La(L^{Bu})]$ from that of $[Cu_3Tb(L^{Bu})]$ removes the contribution of the Cu^{II}−Cu^{II} interaction (also ferromagnetic in $[Cu_3Tb(L^{Bu})]$, as suggested by the ab initio calculations; *vide infra*), the $[Cu_3]$ paramagnetism, and the intrinsic contribution of the Tb^{III} ion. The resulting difference plot (Figure 3) exhibits a minimum at room
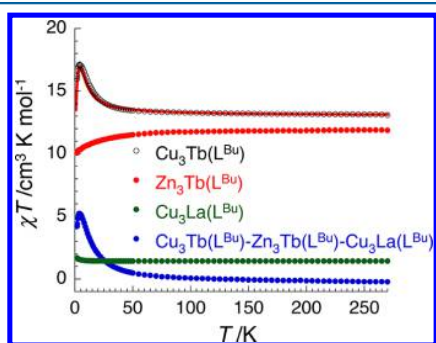

Figure 3. Temperature dependence of χT (with χ defined as molar magnetic susceptibility equal to M/H per mole of $[M_3Ln(L^{Bu})]$) at 1000 Oe for $[Cu_3Tb(L^{Bu})]$ (black, open circle), $[Zn_3Tb(L^{Bu})]$ (red circle), and $[Cu_3La(L^{Bu})]$ (green circle), and the remaining χT product after subtraction of the two analogue contributions from $[Cu_3Tb(L^{Bu})]$ (blue circle). The solid red line on the $[Cu_3Tb(L^{Bu})]$ data is the best simulation obtained from the ab initio calculations described in the text.

temperature before gradually increasing to a maximum at 3.5 K, confirming that the Cu^{II}−Tb^{III} interaction is ferromagnetic. Given that the 3d−3d and 3d−4f interactions are all ferromagnetic, $[Cu_3Tb(L^{Bu})]$ probably possesses a reasonably large magnetic ground state.

The field dependence of magnetization for $[Cu_3Tb(L^{Bu})]$ was measured to check for the presence of an M versus H hysteresis effect (Figure S4, Supporting Information). Below 10 K, the magnetization increases rapidly at low field before a gradual linear increase at high field. At 1.9 K and 70 kOe, the magnetization does not saturate, but reaches 8.1 μ_B. There is no sign of a hysteresis effect for $[Cu_3Tb(L^{Bu})]$ or for $[Zn_3Tb(L^{Bu})]$ and $[Cu_3La(L^{Bu})]$ (Figure S5, Supporting Information). The M versus H/T plots of the $[Cu_3Tb(L^{Bu})]$ complex are not superposable on a single master curve (Figure S4, Supporting Information), which is consistent with the presence of a significant magnetic anisotropy, as expected for a Tb^{III}-containing species.

The response of $[Cu_3Tb(L^{Bu})]$ to an ac magnetic field was measured to check for the presence of slow relaxation of magnetization. The in-phase component shows strong frequency dependence (Figure 4 and Figure S6, Supporting Information) and, below 6 K, the out-of-phase component becomes nonzero and frequency-dependent (Figure S6, Supporting Information), as expected for an SMM. In the plot of χ'' versus frequency (ν) at various temperatures (Figure 4), maxima are clearly visible within the window of the measurement. Hence, the relaxation time can be determined;
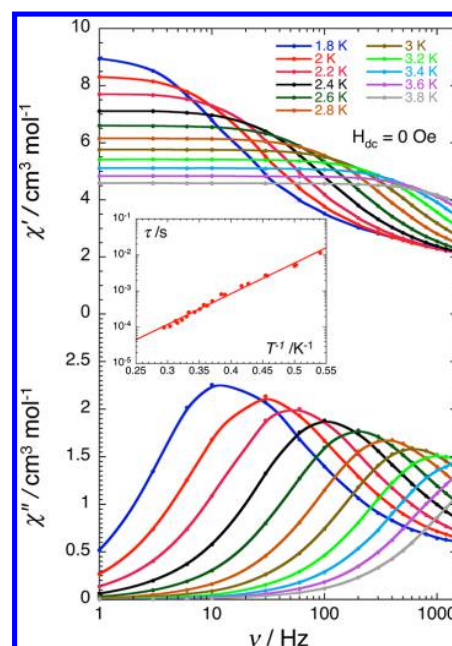

Figure 4. Frequency dependence of the in-phase (top) and out-of-phase (bottom) components of ac susceptibility for $[Cu_3Tb(L^{Bu})]$ at the temperatures indicated in zero dc field. Inset: Relaxation time (τ) versus T^{-1} plot for $[Cu_3Tb(L^{Bu})]$ (red circles) and the Arrhenius fit (red line).

the resulting τ versus T^{-1} plot (Figure 4, inset) fits well to a simple Arrhenius law with Δ_{eff}/k_B = 19.5(5) K and τ_0 = 3.4 × 10^{-7} s. This result indicates that the relaxation of the magnetization is governed by a thermally activated process above 1.8 K.

Ab initio calculations (MOLCAS program package[8a]) were performed in order to investigate local magnetic anisotropy on the Tb^{III} ion (see the Supporting Information for details). Although Tb^{III} is a non-Kramers ion, it was found that the two lowest-lying spin−orbit states are very close in energy, forming an Ising doublet with a small intrinsic gap of 0.24 K (0.17 cm^{-1}). The main magnetic axis (Z) of this doublet passes very close to the $[Cu_3]$ plane (Figure 5). The exchange interactions were evaluated within the Lines model implemented in the POLY_ANISO software,[8b] using the ab initio calculated spin−orbit multiplets on Tb^{III} and isotropic $S = {}^1/_2$ states on the three Cu^{II} ions with a common g = 2.1. All intracomplex exchange couplings were found to be ferromagnetic: $J(Tb−Cu)/k_B$ = +4.34 K (3.02 cm^{-1}); $J(Cu−Cu)/k_B$ = +1.37 K (0.95 cm^{-1}), whereas the intermolecular interaction was weakly antiferromagnetic zJ/k_B = −0.018 K (0.012 cm^{-1}). As illustrated by Figure 3 and Figure S4 (Supporting Information), an excellent agreement between the measured and calculated magnetic properties is found for $[Cu_3Tb(L^{Bu})]$.

Although the overall structure of $[Cu_3Tb(L^{Bu})]$ is very similar to that of the previously studied $[Cu_3Tb(L^{Pr})]$,[4c,d] the ligand field of the Tb^{III} is completely different as two, not one, NO_3^- anions coordinate to the Tb^{III} axial sites in the present complex. This, combined with the modified equatorial ligand field imposed by the larger macrocycle, is probably the key reason for the high axiality of $[Cu_3Tb(L^{Bu})]$, which is, in turn, reflected in a much smaller tunneling gap of the ground Ising doublet (see Table 1 and Table S1, Supporting Information).
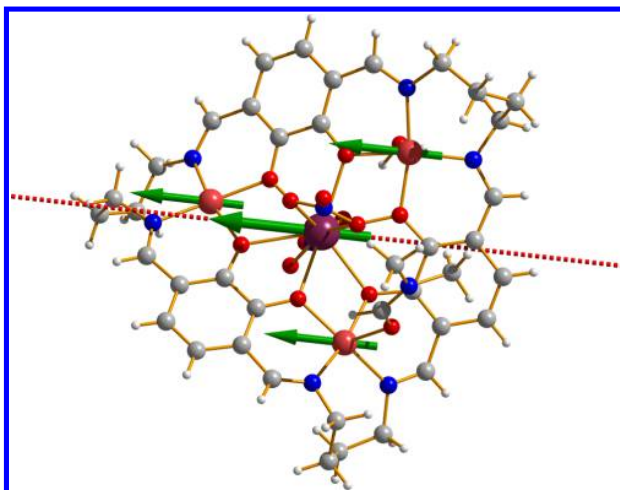
Figure 5. Orientation of the anisotropic axis of the ground Ising doublet on Tb^{III} (red dashed line; at 18.67° to [Cu$_3$] plane, cf 2.22° in [Cu$_3$Tb(L^{Pr})]).[4d] Local magnetizations of the Cu^{II} and Tb^{III} ions are shown by green arrows.

Table 1. Comparison of Five Low-Lying Level Energies [in K (cm^{-1})] Corresponding to the Free Ion J = 6 Multiplet of the Central Tb^{III} Ion in [Cu$_3$Tb(L^{Pr})] and [Cu$_3$Tb(L^{Bu})]^a

[Cu$_3$Tb(L^{Pr})][4d]	[Cu$_3$Tb(L^{Bu})]
0.000	**0.000**
6.11 (4.25)	**0.25 (0.17)**
85.60 (59.50)	60.52 (42.06)
131.40 (91.32)	109.41 (76.04)
146.79 (102.02)	124.76 (86.71)

^{a}The states defining the axiality are shown in bold: the axiality of Tb^{III} ion increases with the decrease of the energy gap.

The low-lying exchange energy levels, exchange coupling constants, and g tensors of the exchange Kramers doublets for the two complexes are compared in Table S2 (Supporting Information). The transverse g$_X$ and g$_Y$ components for the ground exchange Kramers doublet are almost 40 times smaller for [Cu$_3$Tb(L^{Bu})] than for [Cu$_3$Tb(L^{Pr})]. Hence, the transverse Zeeman splitting is small enough in [Cu$_3$Tb(L^{Bu})] to reduce quantum tunneling of magnetization (QTM), leading to *quantifiable* slow relaxation of magnetization in zero dc field (Figure 4), whereas it is expected to be much larger in [Cu$_3$Tb(L^{Pr})], resulting in fast QTM that prevents quantification of the relaxation time in our experimental windows of temperature and ac frequency.[4] The calculated energy of the first excited exchange Kramers doublet in [Cu$_3$Tb(L^{Bu})] is 12 K, which is close to the Arrhenius barrier extracted from the ac susceptibility data (Figure 4).

CONCLUSIONS

Subtle manipulation of the equatorially coordinated macrocycle, deliberately increasing the cavity size by three atoms, from (L^{Pr})$^{6-}$ to (L^{Bu})$^{6-}$, has dramatically improved the SMM behavior of [Cu$_3$Tb(L^{Pr})]. In the resulting complex, [Cu$_3$Tb(L^{Bu})], the modified equatorial field strength leads to the oblate Tb^{III} ion binding *two* nitrate anions in the apical sites, increasing its axiality. This complex is a rare example of a macrocyclic 3d−4f SMM, and the first of this type to exhibit slow relaxation in *zero dc field* that has been experimentally

quantified with an Arrhenius law, so, as it was designed to be, it is the best such SMM reported to date.

EXPERIMENTAL SECTION

General. 1,4-Diformyl-2,3-dihydroxybenzene (1) was prepared according to a synthesis developed in the Brooker group, with advice from Prof. M. MacLachlan (UBC), which is very similar to the procedure published subsequently.[8] All other chemicals were obtained from commercial suppliers and were used as received.

[Cu^{II}$_3$Tb^{III}(L^{Bu})(NO$_3$)$_2$(MeOH)(H$_2$O)](NO$_3$)·3H$_2$O. To a solution of 1 (0.030 g, 0.18 mmol) in methanol (5 mL) was added Cu(OAc)$_2$·H$_2$O (0.036 g, 0.18 mmol) suspended in a solution of Tb(NO$_3$)$_3$·5H$_2$O (0.027 g, 0.06 mmol) in MeOH (10 mL), resulting in a dark brown solution. After stirring this solution for 2 hours and being careful to check that all the Cu(OAc)$_2$·H$_2$O had dissolved, 1,4-diaminobutane (1.8 mL of a 0.1 M standard solution in MeOH) in methanol (5 mL) was added, resulting in a green-brown solution. This reaction was stirred for a further 10 min before being left to stand undisturbed overnight. At this point, diethyl ether was vapor diffused into the solution. The resulting solid was filtered off, air-dried for 1 h, and redissolved in 1:9 DMF/MeOH, and the solution was vapor diffused with diethyl ether giving [Cu^{II}$_3$Tb^{III}(L^{Bu})(NO$_3$)$_2$(MeOH)-(H$_2$O)](NO$_3$)·3H$_2$O as a green powder after drying in air. Green powder (0.037 g, 49%). Found: C, 34.38; H, 3.80; N, 9.78. Calculated for Cu$_3$TbC$_{37}$H$_{48}$N$_9$O$_{20}$: C, 34.49; H, 3.76; N, 9.89. IR (FT-ATR diamond anvil) $\bar{\nu}$/cm^{-1}: 1613 (m); 1523 (w); 1454 (m); 1384 (m); 1325 (s); 1241 (m); 1192 (m); 1177 (m); 1098 (w); 1036 (w); 1006 (w); 847 (w); 778 (w); 730 (m); 641 (w); 597 (m); 562 (w); 476 (m). A single crystal of [Cu$_3$Tb^{III}(L^{Bu})(NO$_3$)$_2$(DMF)(H$_2$O)]-(NO$_3$)·DMF, suitable for X-ray crystallography, was grown by vapor diffusion of diethyl ether into a solution of [Cu^{II}$_3$Tb^{III}(L^{Bu})(NO$_3$)$_2$-(MeOH)(H$_2$O)](NO$_3$)·3H$_2$O in 1:1 DMF/MeOH.

[Cu^{II}$_3$La^{III}(L^{Bu})(NO$_3$)$_2$(MeOH)$_2$(H$_2$O)$_2$](NO$_3$)·H$_2$O·DMF. Prepared in an analogous manner to [Cu$_3$Tb(L^{Bu})], but using La(NO$_3$)$_3$·6H$_2$O instead of Tb(NO$_3$)$_3$·5H$_2$O. Green powder (0.047 g, 59%). Found: C, 36.31; H, 4.28; N, 10.44. Calculated for Cu$_3$LaC$_{40}$H$_{53}$N$_{10}$O$_{20}$: C, 36.30; H, 4.04; N, 10.58. IR (FT-ATR diamond anvil) $\bar{\nu}$/cm^{-1}: 1614 (m); 1518 (w); 1454 (m); 1400 (m); 1326 (s); 1240 (m); 1193 (m); 1176 (w); 1099 (w); 1035 (w); 1005 (w); 850 (w); 774 (w); 734 (m); 644 (w); 601 (m); 561 (w); 479 (m). A single crystal of [Cu$_3$La(L^{Bu})(NO$_3$)$_2$(MeOH)$_3$](NO$_3$), suitable for X-ray crystallography, was grown by vapor diffusion of diethyl ether into a solution of [Cu^{II}$_3$La^{III}(L^{Bu})(NO$_3$)$_2$(MeOH)$_2$(H$_2$O)$_2$](NO$_3$)·H$_2$O·DMF in MeOH.

[Zn^{II}$_3$Tb^{III}(L^{Bu})(NO$_3$)$_3$]·MeOH·H$_2$O·DMF. To a solution of 1 (0.030 g, 0.18 mmol) in methanol (5 mL) was added a solution of Zn(OAc)$_2$·2H$_2$O (0.040 g, 0.18 mmol) and Tb(NO$_3$)$_3$·5H$_2$O (0.027 g, 0.06 mmol) in MeOH (10 mL), resulting in an orange solution. After stirring this solution for 10 min, 1,4-diaminobutane (1.8 mL of a 0.1 M standard solution in MeOH) was added. This reaction was stirred for a further 10 min before being left to stand undisturbed overnight. At this point, diethyl ether was vapor diffused into the solution. The resulting solid was filtered off, air-dried for 1 h, and redissolved in 1:9 DMF/MeOH, and the solution was vapor diffused with diethyl ether, giving Zn^{II}$_3$Tb^{III}(L^{Bu})(NO$_3$)$_3$·MeOH·H$_2$O·DMF after drying in air. Orange powder (0.067 g, 85%). Found: C, 36.41; H, 3.88; N, 10.97. Calculated for Zn$_3$TbC$_{40}$H$_{49}$N$_{10}$O$_{18}$: C, 36.59; H, 3.76; N, 10.67. IR (FT-ATR diamond anvil) $\bar{\nu}$/cm^{-1}: 1656 (m); 1615 (s); 1516 (m); 1457 (m); 1428 (m); 1415 (m); 1386 (m); 1335 (s); 1325 (s); 1237 (m); 1226 (m); 1191 (m); 1172 (s); 1116 (m); 1907 (m); 1074 (m); 1050 (m); 1036 (m); 1007 (m); 996 (m); 856 (m); 730 (s).

X-ray Crystallography. Data were collected on a Bruker Kappa Apex II area detector diffractometer at 89−90 K using graphite monochromated Mo Kα radiation (λ = 0.71073 Å). Both data sets were absorption-corrected using SCALE. The structures were solved using SHELXS-97 and refined against F^2 using all data by full-matrix least-squares techniques with SHELXL-97.[9] Details of the refinements are provided in the Supporting Information. Crystallographic data

have been deposited with the Cambridge Crystallographic Data Centre (CCDC 908288 and 908289).

Crystal Data for [Cu$_3$La(L^{Bu})(NO$_3$)$_2$(MeOH)$_3$](NO$_3$). Monoclinic, P2$_1$/n, brown block, a = 10.4983(7) Å, b = 36.136(3) Å, c = 12.6822(9) Å, β = 110.807(4)°, V = 4497.5(6) Å^3, Z = 4, T = 90 K. The structure was solved by direct methods using SHELXS-97[10] and refined against all F^2 data (SHELXL[11]) to R1 of 0.0841 for 5810 data with $F > 4\sigma(F)$; wR2 = 0.2176, GOF = 1.044 for all 8201 unique reflections.

Crystal Data for [Cu$_3$Tb(L^{Bu})(NO$_3$)$_2$(DMF)(H$_2$O)](NO$_3$)·DMF. Triclinic, P$\overline{1}$, brown block, a = 12.1520(9) Å, b = 15.4239(13) Å, c = 17.2251(14) Å, α = 65.999(3)°, 72.507(3)°, γ = 67.956(3)°, V = 2691.7(4) Å^3, Z = 2, T = 90 K. The structure was solved by direct methods using SHELXS-97[10] and refined against all F^2 data (SHELXL[11]) to R1 of 0.0841 for 5810 data with $F > 4\sigma(F)$; wR2 = 0.2176, GOF = 1.066 for all 10 960 unique reflections.

■ ASSOCIATED CONTENT

⑤ Supporting Information

Description and figure of the structure of [Cu$_3$La(L^{Bu})] and additional refinement details, additional magnetic data, and ab initio results. This material is available free of charge via the Internet at http://pubs.acs.org.

■ AUTHOR INFORMATION

Corresponding Author

*E-mail: sbrooker@chemistry.otago.ac.nz.

Notes

The authors declare no competing financial interest.

■ ACKNOWLEDGMENTS

■ REFERENCES

(1) Gatteschi, D.; Sessoli, R.; Villain, F. *Molecular Nanomagnets*; Oxford University Press: Oxford, U.K., 2006.

(2) (a) Sessoli, R.; Powell, A. K. *Coord. Chem. Rev.* **2009**, *253*, 2328. (b) Gatteschi, D.; Sessoli, R.; Cornia, A. *Chem. Commun.* **2000**, 725. (c) Aromí, G.; Brechin, E. K. *Struct. Bonding (Berlin, Ger.)* **2006**, *122*, 1. (d) Glaser, T. *Chem. Commun.* **2011**, *47*, 116. (e) Kostakis, G. E.; Hewitt, I. J.; Ako, A. M.; Mereacre, V.; Powell, A. K. *Philos. Trans. R. Soc. London, Ser. A* **2010**, *368*, 1509. (f) Ishikawa, N. *Polyhedron* **2007**, *26*, 2147. (g) Murrie, M. *Chem. Soc. Rev.* **2010**, *39*, 1986. (h) Rinehart, J. D.; Long, J. R. *Chem. Sci.* **2011**, *2*, 2078.

(3) Winpenny, R. E. P. *J. Chem. Soc., Dalton Trans.* **2002**, 1.

(4) (a) Feltham, H. L. C.; Lan, Y.; Klöwer, F.; Ungur, L.; Chibotaru, L. F.; Powell, A. K.; Brooker, S. *Chem.—Eur. J.* **2011**, *17*, 4362. (b) Feltham, H. L. C.; Klöwer, F.; Cameron, S. A.; Larsen, D. S.; Lan, Y.; Tropiano, M.; Faulkner, S.; Powell, A. K.; Brooker, S. *Dalton Trans.* **2011**, *40*, 11425. (c) Feltham, H. L. C.; Clérac, R.; Powell, A. K.; Brooker, S. *Inorg. Chem.* **2011**, *50*, 4232. (d) Feltham, H. L. C.; Clérac, R.; Ungur, L.; Vieru, V.; Chibotaru, L. F.; Powell, A. K.; Brooker, S. *Inorg. Chem.* **2012**, *51*, 10603.

(5) Yamashita, A.; Watanabe, A.; Akine, S.; Nabeshima, T.; Nakano, M.; Yamamura, T.; Kajiwara, T. *Angew. Chem., Int. Ed.* **2011**, *50*, 4016.

(6) Addison, A. W.; Rao, T. N.; Reedijk, J.; van Rijn, J.; Vershoor, G. C. *J. Chem. Soc., Dalton Trans.* **1984**, 1349.

(7) van Vleck, J. H. *The Theory of Electric and Magnetic Susceptibility*; Oxford University Press: Oxford, U.K., 1932.

(8) Akine, S.; Taniguchi, T.; Nabeshima, T. *J. Am. Chem. Soc.* **2006**, *128*, 15765.

(9) Sheldrick, G. M. *Acta Crystallogr., Sect. A* **2008**, *A64*, 112.

(10) Sheldrick, G. M. *Meth. Enzymol.* **1997**, *276*, 628.

(11) Sheldrick, G. M.; Schneider, T. R. *Meth. Enzymol.* **1997**, *277*, 319.